Electrochemistry Communications 159 (2024) 107655

Contents lists available at ScienceDirect

Electrochemistry Communications

journal homepage: www.elsevier.com/locate/elecom

Short Communication

Performance of a PEM fuel cell cathode catalyst layer under oscillating potential and oxygen supply

Andrei Kulikovsky

Forschungszentrum Jülich GmbH, Theory and Computation of Energy Materials (IEK–13), Institute of Energy and Climate Research, D–52425 Jülich, Germany

ARTICLE INFO

Keywords:
PEM fuel cell
Catalyst layer
Impedance
Modeling

ABSTRACT

A model for impedance of a PEM fuel cell cathode catalyst layer under simultaneous application of potential and oxygen concentration harmonic perturbations is solved. The solution demonstrates strong lowering of the layer impedance under increase in the amplitude of oxygen concentration perturbation. Small in–phase oscillations of the overpotential and oxygen concentration lead to formation of a sub–layer with negligible oxygen transport loss. Working as an ideal non–polarizable electrode, this sub–layer dramatically reduces the system impedance.

1. Introduction

Electrochemical impedance spectroscopy (EIS) has proven to be a unique non–destructive and non–invasive tool for fuel cells characterization [1]. In its classic variant, EIS is based on application of a small–amplitude harmonic perturbation of the cell current or potential and measuring the response of the cell potential or current, respectively. In recent years, there has been interest in alternative techniques based on application of pressure (Engebretsen et al.[2], Shirsath et al.[3], Schiffer et al.[4], Zhang et al.[5]) or oxygen concentration (Sorrentino et al.[6–8]) perturbation to the cell and measuring the response of electric variable (potential or current), keeping the second electric variable constant.

Application of pressure oscillations at the cathode channel inevitably leads to flow velocity oscillations (FVO) [9]. Kim et al.[10] and Hwang et al.[11] demonstrated experimentally dramatic improvement of PEM fuel cell performance under applied FVO. The effect of FVO on the cell performance was more pronounced with lower static flow rates and with increasing the FVO amplitude [10]. In [10,11], the effect has been attributed to improvement of diffusive oxygen transport through the cell due to FVO. Kulikovsky [12,13] developed a simplified analytical model for impedance of the cell subjected to simultaneous oscillations of potential and air flow velocity. The model has shown reduction of the cell static resistivity upon increase of the FVO amplitude. Yet, however, due to system complexity, the mechanism of cell performance improvement is not fully understood.

Below, a much simpler system (PEM fuel cell cathode catalyst layer) subjected to oscillating in–phase potential and oxygen supply is considered. Analytical model for the CCL impedance under these conditions is solved. The result demonstrates the effect of impedance reduction due to oscillating oxygen supply. In–phase oxygen concentration and overpotential oscillations strongly reduce oxygen transport losses in part of the cathode catalyst layer (CCL) at the CCL/gas diffusion layer (GDL) interface which leads to dramatic decrease of the system impedance.

2. Model

Consider a problem for CCL impedance under simultaneously oscillating potential and oxygen supply (Fig. 1). For simplicity, we will assume that the proton transport is fast. The model is based on two equations: the proton charge conservation

$$C_{dl}\frac{\partial \eta}{\partial t}+\frac{\partial j}{\partial x}=-i_*\left(\frac{c}{c_{ref}}\right)\exp\left(\frac{\eta}{b}\right) \tag{1}$$

and the oxygen mass transport equation

$$\frac{\partial c}{\partial t}-D_{ox}\frac{\partial^2 c}{\partial x^2}=-\frac{i_*}{4F}\left(\frac{c}{c_{ref}}\right)\exp\left(\frac{\eta}{b}\right). \tag{2}$$

Here, x is the distance through the CCL, C_{dl} is the double layer capacitance, η is the positive by convention ORR overpotential, t is time, j is the local proton current density, i_* is the ORR volumetric exchange current density, c_{ref} is the reference oxygen concentration, and b is the ORR Tafel slope. Introducing dimensionless variables

E-mail address: A.Kulikovsky@fz-juelich.de.

https://doi.org/10.1016/j.elecom.2023.107655
Received 13 October 2023; Received in revised form 20 December 2023; Accepted 20 December 2023
Available online 28 December 2023

Nomenclature

~	Marks dimensionless variables
b	ORR Tafel slope, V
C_{dl}	Double layer volumetric capacitance, F cm^{-3}
c	Oxygen molar concentration, mol cm^{-3}
c_{ref}	Reference oxygen concentration, mol cm^{-3}
D_{ox}	Oxygen diffusion coefficient in the CCL, cm^2 s^{-1}
F	Faraday constant, C mol^{-1}
f	Frequency, Hz
G	Dimensionless concentration admittance $\tilde{c}^1/\tilde{\eta}_1^1$
j	Local proton current density, A cm^{-2}
i	Imaginary unit
i_*	ORR volumetric exchange current density, A cm^{-3}
k	Concentration amplitude factor, Eq. (7)
l_t	Catalyst layer thickness, cm
R	Static resistivity, Ω cm^2
R_{ct}	Static charge transfer resistivity, Ω cm^2
t	Time, s
x	Coordinate through the cell, cm
Z	CCL impedance, Ω cm^2

Subscripts:

RC	parallel RC–circuit impedance
W	Warburg finite–length impedance
0	membrane/CCL interface
1	CCL/GDL interface

Superscripts:

0	Steady–state value
1	Small perturbation amplitude

Greek:

η	ORR overpotential, positive by convention, V
η_1^1	Amplitude of applied overpotential perturbation, V
μ	Dimensionless parameter, Eq. (5)
ϕ	Dimensionless parameter, Eq. (10)
ω	Angular frequency of the AC signal, s^{-1}

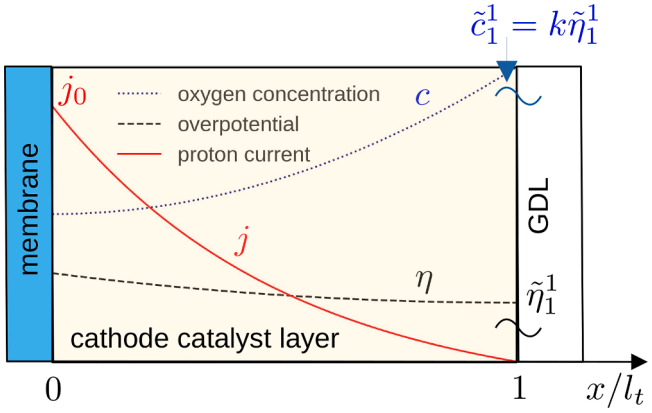

Fig. 1. Schematic of the cathode catalyst layer and the typical static shapes of the oxygen concentration, proton current density and overpotential in the layer. In–phase harmonic perturbations of the dimensionless overpotential $\tilde{\eta}_1^1$ and oxygen concentration $\tilde{c}_1^1$ are applied at the CCL/GDL interface.

$$\tilde{x} = \frac{x}{l_t},\quad \tilde{t} = \frac{ti_*}{C_{dl}b},\quad \tilde{c} = \frac{c}{c_{ref}},\quad \tilde{\eta} = \frac{\eta}{b},\quad \tilde{j} = \frac{j}{i_* l_t},$$
$$\tilde{D}_{ox} = \frac{4FD_{ox}c_{ref}}{i_* l_t^2},\quad \tilde{Z} = \frac{Zi_* l_t}{b},\quad \tilde{\omega} = \frac{\omega C_{dl} b}{i_*}, \tag{3}$$

where $\tilde{\omega}$ is the angular frequency of applied AC signal, $\tilde{Z}$ is the CCL impedance, Eqs. (1), (2) take the form

$$\frac{\partial\tilde{\eta}}{\partial\tilde{t}} + \frac{\partial\tilde{j}}{\partial\tilde{x}} = -\tilde{c}\exp\tilde{\eta} \tag{4}$$

$$\mu^2\frac{\partial\tilde{c}}{\partial\tilde{t}} - \tilde{D}_{ox}\frac{\partial^2\tilde{c}}{\partial\tilde{x}^2} = -\tilde{c}\exp\tilde{\eta},\quad \mu \equiv \sqrt{\frac{4Fc_{ref}}{C_{dl}b}}. \tag{5}$$

Linearization and Fourier transform of Eqs. (4), (5) lead to the system of linear equations relating the perturbation amplitudes $\tilde{\eta}_1^1(\tilde{\omega}), \tilde{j}^1(\tilde{x},\tilde{\omega})$ and $\tilde{c}^1(\tilde{x},\tilde{\omega})$ (Ref.[14]):

$$\frac{\partial\tilde{j}^1}{\partial\tilde{x}} = -\exp\left(\tilde{\eta}^0\right)\left(\tilde{c}^1 + \tilde{c}_1^0\tilde{\eta}_1^1\right) - i\tilde{\omega}\tilde{\eta}_1^1,\quad \tilde{j}^1\left(1\right) = 0 \tag{6}$$

$$\tilde{D}_{ox}\frac{\partial^2\tilde{c}^1}{\partial\tilde{x}^2} = \exp\left(\tilde{\eta}^0\right)\left(\tilde{c}^1 + \tilde{c}_1^0\tilde{\eta}_1^1\right) + i\mu^2\tilde{\omega}\tilde{c}^1,$$
$$\left.\frac{\partial\tilde{c}^1}{\partial\tilde{x}}\right|_{\tilde{x}=0} = 0,\quad \tilde{c}^1(1) = k\tilde{\eta}_1^1 \tag{7}$$

where the superscripts 0 and 1 mark the static variables and the small perturbation amplitudes, respectively, $\tilde{c}_1^0$ is the static oxygen concentration at the CCL/GDL interface, $k \geqslant 0$ is the constant model parameter, $\tilde{\eta}_1^1$ is the amplitude of applied overpotential perturbation.

The boundary condition for Eq. (6) means zero proton current through the CCL/GDL interface. The left boundary condition for Eq. (7) expresses zero oxygen flux in the membrane. The feature of this problem is the right boundary condition for Eq. (7) meaning external control of oxygen concentration perturbation $\tilde{c}^1$ at the CCL/GDL interface: $\tilde{c}^1(1)$ varies in–phase with the overpotential perturbation $\tilde{\eta}_1^1$. Note that the perturbations of applied cell potential and *positive* overpotential have different signs, assuming that the electron conductivity of the cell components is much larger than the CCL proton conductivity.

Due to fast proton transport, $\tilde{\eta}_1^1$ is nearly independent of $\tilde{x}$. For simplicity we will also assume that the variation of static oxygen concentration along $\tilde{x}$ is small: $\tilde{c}^0 \simeq \tilde{c}_1^0$. Note that the account of a static oxygen concentration non–uniformity qualitatively does not change the effects below. The procedure of Eqs.(6), (7) solution is quite analogous to the one described in [14]; it leads to the CCL impedance

$$\tilde{Z} = \frac{\tilde{Z}_{RC}}{(\tilde{j}_0/\tilde{c}_1^0)(k\tilde{Z}_{RC} + \tilde{j}_0)\tilde{Z}_W + (\tilde{j}_0\mu^2 + \tilde{Z}_{RC})i\tilde{\omega}}, \tag{8}$$

where j_0 is the cell current density, $\tilde{Z}_{RC}$ is the parallel RC–circuit (faradaic) impedance, $\tilde{Z}_W$ is the Warburg–like oxygen transport impedance:

$$\tilde{Z}_{RC} = \frac{\tilde{j}_0}{\tilde{c}_1^0} + i\mu^2\tilde{\omega},\quad \tilde{Z}_W = \frac{\tanh\left(\sqrt{\tilde{Z}_{RC}/\tilde{D}_{ox}}\right)}{\sqrt{\tilde{Z}_{RC}/\tilde{D}_{ox}}}, \tag{9}$$

and the static polarization equation $\tilde{j}_0 = \tilde{c}_1^0\exp\tilde{\eta}^0$ has been used to eliminate $\exp\tilde{\eta}^0$.

The CCL impedance, Eq. (8), for the current density of 100 mA cm^{-2} and the indicated values of parameter k is shown in Fig. 2. The other parameters are listed in Table 1. Note that to emphasize the effect, the

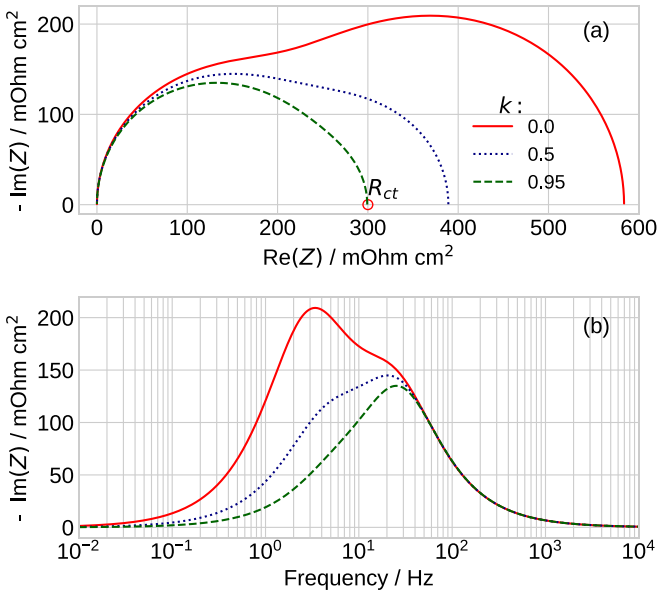

Fig. 2. (a) Nyquist spectra of the CCL, Eq. (8), for the indicated values of parameter k. The other parameters are listed in Table 1. The point R_{ct} indicates the static charge–transfer resistivity b/j_0. (b) The frequency dependence of impedances in (a).

Table 1
The cell parameters used in calculations. Parameter D_{ox} is taken to be small to emphasize the effect of oxygen transport in the CCL.

Tafel slope b, V	0.03
Double layer capacitance C_{dl}, F cm^{-3}	20
Exchange current density i_*, A cm^{-3}	10^{-3}
Oxygen diffusion coefficient in the CCL, D_{ox}, cm^2 s^{-1}	$1{\cdot}10^{-5}$
Catalyst layer thickness l_t, cm	$10{\cdot}10^{-4}$
Cell temperature T, K	273 + 80
Cathode pressure, bar	1.5
Cathode relative humidity, %	50
Cell current density j_0, A cm^{-2}	0.1

CCL oxygen diffusivity is taken to be very low, $D_{ox} = 10^{-5}$ cm^2 s^{-1}.

The Nyquist spectrum corresponding to $k = 0$ (no concentration perturbation at the CCL/GDL interface) consists of two partly overlapping arcs, of which the left one is due to charge transfer and the right one is due to oxygen transport (Fig. 2a). In Fig. 2b, the left peak of $-\Im(Z)$ (red curve) corresponds to the oxygen transport and the right shoulder is due to the faradaic reaction.

The perturbation of oxygen concentration at the CCL/GDL interface dramatically changes the spectra. With the growth of k, the oxygen transport arc strongly decreases showing strong lowering of the oxygen transport loss (Fig. 2). The reduction of transport impedance lowers the CCL static resistivity $\widetilde{R}$ (Fig. 2a). Calculation of Eq. (8) limit as $\widetilde{\omega}\to 0$ gives

$$\widetilde{R} = \frac{\phi\coth(\phi)}{\widetilde{j}_0(1 + k/\widetilde{c}_1^0)}, \quad \phi \equiv \sqrt{\frac{\widetilde{j}_0}{\widetilde{c}_1^0 \widetilde{D}_{ox}}} \tag{10}$$

which decreases with the growth of k.

To understand the effect, it is advisable to check what happens to the phase shift between the oxygen concentration $\widetilde{c}^1$ and overpotential $\widetilde{\eta}_1^1$ (the phase angle of $G(\widetilde{x}) = \widetilde{c}^1/\widetilde{\eta}_1^1$) at $k \geqslant 0$ (Fig. 3a). At $k = 0$, there is a large phase shift between $\widetilde{c}_1$ and $\widetilde{\eta}_1^1$, excluding a single point at $\widetilde{x} = 1$, where $\widetilde{c}^1 = 0$. With $k = 0.5$, a finite–thickness domain forms, where $\widetilde{c}^1$

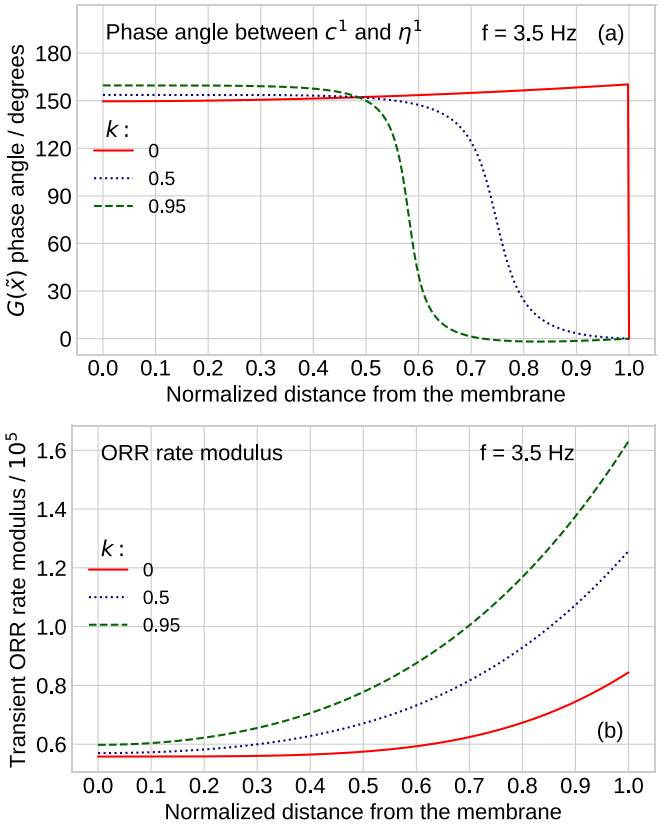

Fig. 3. (a) The phase angle of $G = \widetilde{c}^1/\widetilde{\eta}_1^1$ (between oxygen concentration and overpotential) vs distance $\widetilde{x}$ through the CCL at the frequency of 3.5 Hz corresponding to position of the transport peak in Fig. 2b (red curve). (b) The modulus of the transient ORR rate.

and $\widetilde{\eta}_1^1$ oscillate almost in–phase, and with $k = 0.95$ this domain of zero phase shift increases (Fig. 3a). Zero phase angle between $\widetilde{\eta}_1^1$ and $\widetilde{c}^1$ means small or no oxygen transport losses in this domain.

Fig. 3b shows the modulus of the ORR rate perturbation. In the domain with low oxygen transport loss, the ORR rate strongly increases. Thus, at $k > 0$, a sub–layer at the CCL/GDL interface forms, which works as an ideal non–polarizable electrode with fast oxygen transport and large ORR rate. This sub–layer significantly reduces the CCL impedance.

Further increase in k above 0.95 changes the sign of the G phase angle at the membrane interface, meaning formation of inductive loop in the Nyquist spectrum. In this state, the static resistivity drops below the static charge–transfer value $R_{ct} = b/j$; this regime deserves special consideration and it is not discussed here. The limiting value $k_{\rm lim}$ at which $\widetilde{R} = \widetilde{R}_{ct} = 1/\widetilde{j}_0$ is

$$k_{\rm lim} = \widetilde{c}_1^0(\phi\coth(\phi) - 1) \tag{11}$$

A steady state of the CCL resulting from solution of the static version of Eqs. (4), (5) leads to the CCL resistivity corresponding to $k = 0$ in Eq. (10) (the rightmost point of the red curve in Fig. 2a). In this state, small variation of the static oxygen concentration at the CCL/GDL interface leads to a small change in the static resistivity. However, if a small harmonic perturbation c_1^1 varying in–phase with the overpotential oscillations η_1^1 is applied at the CCL/GDL interface, the CCL transforms into quite a different two–layer system, with negligible oxygen transport loss in one of the sub–layers. With the decrease in ω, this new system tends to the steady state with much lower resistivity. A more detailed analysis of such a "post–oscillating" steady state will be provided in a full–length paper.

From practical perspective, in a real fuel cell it is hardly feasible to

directly perturb the oxygen concentration at the CCL/GDL interface in–phase with the overpotential. However, the experiments of Kim et al. [10] and Hwang et al.[11] suggest that the effect could be achieved by perturbing air flow velocity in the channel. Oxygen concentration in the channel can, indeed, be perturbed in–phase with the ORR overpotential by applying pressure and/or flow velocity oscillations. The key problem is to understand how GDL affects the phase angle of the transported oxygen concentration perturbation. Calculations show that in the range of frequencies below 1 Hz, GDL does not change the phase angle of oxygen oscillations (to be published elsewhere). This opens a perspective for practical realization of the effect discussed in the work.

Declaration of Competing Interest

The authors declare that they have no known competing financial interests or personal relationships that could have appeared to influence the work reported in this paper.

Data availability

No data was used for the research described in the article.

References

[1] A. Lasia, Electrochemical Impedance Spectroscopy and its Applications, Springer, New York, 2014.
[2] E. Engebretsen, T.J. Mason, P.R. Shearing, G. Hinds, D.J.L. Brett, Electrochem. Comm. 75 (2017) 60–63, https://doi.org/10.1016/j.elecom.2016.12.014.
[3] A.V. Shirsath, S. Rael, C. Bonnet, L. Schiffer, W. Bessler, F. Lapicque, Curr. Opin. Electrochem. 20 (2020) 82–87, https://doi.org/10.1016/j.coelec.2020.04.017.
[4] L. Schiffer, A.V. Shirsath, S. Raël, F. Lapicque, W.G. Bessler, J. Electrochem. Soc. 169 (2021) 034503, https://doi.org/10.1149/1945-7111/ac55cd.
[5] Q. Zhang, H. Homayouni, B.D. Gates, M. Eikerling, A.M. Niroumand, J. Electrochem. Soc. 169 (2022) 044510, https://doi.org/10.1149/1945-7111/ac6326.
[6] A. Sorrentino, T. Vidakovic-Koch, R. Hanke-Rauschenbach, K. Sundmacher, Electrochim. Acta 243 (2017) 53–64, https://doi.org/10.1016/j.electacta.2017.04.150.
[7] A. Sorrentino, T. Vidakovic-Koch, K. Sundmacher, J. Power Sources 412 (2019) 331–335, https://doi.org/10.1016/j.jpowsour.2018.11.065.
[8] A. Sorrentino, K. Sundmacher, T. Vidakovic-Koch, Energies 13 (2020) 5825, https://doi.org/10.3390/en13215825.
[9] T. Sexl, Z. Phys. 61 (1930) 349–362, https://doi.org/10.1007/BF01340631.
[10] Y.H. Kim, H.S. Han, S.Y. Kim, G.H. Rhee, J. Power Sources 185 (2008) 112–117, https://doi.org/10.1016/j.jpowsour.2008.06.069.
[11] Y.-S. Hwang, D.-Y. Lee, J.W. Choi, S.-Y. Kim, S.H. Cho, P. Joonho, M.S. Kim, J. H. Jang, S.H. Kim, S.-W. Cha, Int. J. Hydrogen Energy 35 (2010) 3676–3683, https://doi.org/10.1016/j.ijhydene.2010.01.064.
[12] A. Kulikovsky, arXiv (2020). arXiv:2008.07101, doi:10.48550/arXiv.2008.07101.
[13] A. Kulikovsky, eTrans. 5 (2021) 100104, https://doi.org/10.1016/j.etran.2021.100104.
[14] A.A. Kulikovsky, Electrochim. Acta 196 (2016) 231–235, https://doi.org/10.1016/j.electacta.2016.02.150.